Zinc-based alloy rapid tooling for sheet metal forming reinforced by SLM steel inlays

Tong Wen (tonywen68@hotmail.com)
Chongqing University https://orcid.org/0000-0003-3266-2212
Longqin Liu
Xu Wang
Yu Zheng
Fan Yang
Yin Zhou

Research Article

Keywords: Sheet metal forming, Rapid tooling, Additive manufacturing, Selective laser melting, Steel inlay

Posted Date: March 9th, 2022

DOI: https://doi.org/10.21203/rs.3.rs-1418247/v1

Abstract

Among the existing rapid and economical sheet metal forming technologies, stamping with a press using soft tools, especially low-melting-point alloy dies, is one of the few methods that can meet the precision requirements in industrial fields such as automobile manufacturing. However, the usability of the method is limited by the low strength of the soft base. The current study proposes a new structure of zinc-based alloy dies for sheet metal forming, where the weak features of the die blocks, such as protruding edges, are reinforced by selective laser melting (SLM) steel inlays imbedded during solid–liquid compound casting. A technical route for fabricating the new tools was developed, and a W-shaped part was formed using an SUS304 sheet with a thickness of 0.32 mm and an Al6061 sheet with a thickness of 1 mm to validate the concept. The experiment and simulation results proved that clearer localized features, such as a smaller radius, can be formed on the workpiece with the reinforcement of steel inlays, while the springback is smaller and the abrasion resistance of the tool is higher. This method can improve the forming quality and durability of traditional soft tools in a convenient and affordable way.

1 Introduction

Conventional sheet metal-forming technologies are mainly suitable for mass production due to the requirement of specific and complicated mechanical tools, which inevitably incurs a long lead time and high material and process costs. Since the 1980s, great effort has been made to meet the demand for the small-lot production of sheet metal parts, and a variety of fast or dieless sheet-forming methods have been proposed and studied extensively. For example, He et al. (2000) [1] discussed the explosive forming of thin-wall semispherical parts, and the design principles of such shell structures and related technological parameters were introduced. Yarlagadda et al. [2] used a combination of stereolithography and nickel eletroforming processes to develop a rapid tool (RT) for the production of sheet metal drawing. The tools were then evaluated by forming components with 0.8-mm aluminum sheets. Yoo and Walczyk [3] studied the design and development of an RT called profiled edge laminate tool, involving the assembly of an array of laminates, with the top edges being simultaneously profiled and beveled according to a CAD model of the intended surfaces. Zhang et al. [4] investigated rapid hard tooling by plasma spraying for injection molding and sheet metal forming. To improve the durability of the tool, composite materials made of ceramic and metal powders were used as the sprayed original mold materials. Male et al. [5] studied plasma-jet forming, and a robotic system was used to manipulate a nontransferred arc plasma torch to locally heat sheet metal. Thermal conductivity was the principal physical property affecting the bending behavior. Lasers can also be used as controllable heat sources to bend metal plates into complex 3D shapes by generating thermal stress in the materials. Kyrsanidi et al. [6] proposed an analytical model for predicting the distortions caused by the laser forming process. Bachmann et al. [7] stated that laser forming can address two notable shortcomings of metal 3D printing, namely, large structures and thin structures. This method has been applied to shell fabrication in the shipbuilding industry. Shulkin et al. [8] developed an eight-point blank holder force control system in a viscous pressure forming (VPF) machine, and Liu et al. [9] confirmed that the formability of a sheet

stretched with VPF is higher than that of a sheet stretched with a hard punch due to the lower interface friction. Liu et al. [10] optimized cushion conditions in micro multipoint sheet forming to obtain better surface quality and thickness distribution. Li et al. [11] used a sparse multipoint flexible forming tool to obtain doubly curved shapes of AA2050-T34 plates in creep age forming.

In recent years, flexible forming methods based on CNC technologies, especially incremental sheet forming and its variations, have received widespread attention. For example, Wu et al. [12] proposed a multistep strategy to solve the local thinning problem of parts with steep walls in single point incremental forming (SPIF); Milutinovic et al. [13] studied the geometric and physical properties of a stainless steel denture framework made by SPIF; Wen et al. [14] modified bar tools in SPIF to form thin-walled parts with nonbiaxial stretching deformation features; Jurisevic et al. [15] applied laminated supporting tools in water jet incremental sheet metal forming; Cui et al. [16] studied electromagnetic incremental forming (EMIF), where the part is shaped by accumulating the local deformations caused by the small discharge energy at high speed. Wang et al. [17] investigated the friction stir-assisted SPIF of aluminum alloy sheets to achieve higher formability and surface quality.

In the existing technologies for rapid and economical sheet metal forming, stamping with soft tools has the same deformation mode as conventional stamping processes, and it is one of the few methods that can meet the quality and precision requirements in industrial fields such as automobile manufacturing. This is important for sheet metal parts that need functional testing, since they must be representative of the actual performance. Various materials are used in soft tooling, including low-melting-point alloys, resins, and concrete. For instance, Durgun et al. [18] utilized bismuth MCP 137 alloy, a recyclable low-melting-point alloy, to manufacture rapid tools for producing sheet metal parts. More inaccuracies occurred during the tool-making stage rather than during press forming, and the usable tool life was significantly shortened by harder and thicker steel sheets.

The lack of strength of soft tools makes it difficult to form the required clear and delicate geometric features, and the usability is limited. In this situation, much work has been done to improve the strength and durability of soft tools. For example, Kuo and Li [19] examined the effect of ZrO_2 addition on the mechanical properties of epoxy resin dies for sheet metal forming. They confirmed that an epoxy resin material filled with 30 wt% ZrO_2 particles had the highest wear resistance. Kleiner et al. [20] investigated sheet metal hydroforming dies made of ultrahigh performance concrete (UHPC) with a compressive strength of approx. 250 MPa and a Young's modulus of approx. 50 GPa. Although the formed parts had good shape accuracy, the required internal pressure could not be withstood by the UHPC die in the case of small part radii.

Overall, as Schuh et al. [21] summarized, "currently there is no suitable technology for the economic production of deep drawn parts in low quantities" due to the various drawbacks of existing technologies for rapid sheet metal forming. To improve the usability of soft tools, this paper proposes a new structure of a zinc alloy die by combining traditional soft tooling and additive manufacturing (AM) or 3D printing

(3DP) technologies. A technical route for developing the new tool was constructed, and a W-shaped part with sharp corners was formed to evaluate the feasibility of the method.

2 Technical Route For Developing Soft Tools Reinforced By Steel Inlay

As shown in Fig. 1, the new zinc alloy die adopts the conventional configuration of stamping dies; however, to improve the bearing capacity, weak positions, such as the protruding ridges on the die blocks, are reinforced by steel inlays fabricated by AM techniques – especially the selective laser melting (SLM) process, which can directly make metal parts with nearly full density and good mechanical properties.

Figure 2 demonstrates the manufacturing procedure of the new tool. First, a traditional soft die made by a low-melting-point alloy for stamping on a press was designed according to the required part. Then, numerical simulation was conducted to analyze the stamping process. The stress distributions and elastic–plastic deformations of the upper and lower die blocks were used to determine the locations and geometries of the inlays.

Generally, the maximum forming load appears at the bottom dead center of the press; therefore, the inlay(s) can be determined based on the stress distributions (e.g., the von Mises stress) in the die blocks at that moment. The regions with the largest stress – mostly located at the convex edges – can be replaced by steel inlays. Other factors, including the equipment capability and cost, should also be considered. Then, the improved die blocks can be input into FEM software to analyze the stamping process again, and the technical and economic rationality of the new tool can be comprehensively evaluated.

The die blocks are bimetal composite structures made by solid–liquid compound casting, where two metals or alloys are joined by pouring one liquid metal onto or around another solid metal. Due to the high flexibility of AM technologies, the inlay design has much more freedom to meet technical and economic demands. For example, differentiated structures can be adopted in different areas. Specifically, the working surfaces are dense and smooth to guarantee forming quality, while the interfaces connecting the zinc base can employ a rugged or porous pattern to increase the bonding strength.

The casting cores can also be made by the 3DP of a resin. With the boom of AM technologies in recent years, the cost has significantly decreased. Meanwhile, most materials of new tools are recyclable; thus, the overall cost can be controlled within a reasonable level. For the time cycle, compared with that of conventional zinc-based rapid dies, the total processing time of the new tool does not increase much, although the design and fabrication of inlays are added, since many works can be carried out simultaneously.

3 Experiment And Theoretical Analysis Method

Figure 3 illustrates the target workpiece and the 3D model of the stamping die. The materials of the blanks used for forming are Al6061 sheets with a thickness of 1 mm and SUS304 sheets with a thickness of 0.32 mm. The inside radius of the middle corner of the W-shaped part is intentionally set to a small value of 1 mm, which is hard to form with a normal soft die.

Zamak5, a low-melting-point alloy, was used to make the die blocks by a casting process. The inlays were made of nickel-based alloy IN625 by the SLM process. The mechanical properties of the abovementioned materials were obtained by uniaxial tensile tests at room temperature with a tensile speed of 5 mm/s. Figure 4 shows the stress–strain curves of the materials based on experiments, and Table 1 shows the mechanical parameters.

The forming operations were carried out on a WDW-100 universal material testing machine. During forming, the maximum load was set to several constants, namely, 30 kN, 50 kN and 80 kN. When the set value of the maximum load was reached, the forming operation stopped. A maximum load of 100 kN was also used in the theoretical analysis. To guarantee repeatability and consistency, each case was repeated at least three times.

Numerical simulations were carried out in the FEM software of Abaqus. The dynamic explicit method was used in the calculation of the stamping stage, while the static implicit algorithm was used in the calculation of springback after forming. In theory, the deformations of the steel inlay and zinc base should be elastic during the stamping processes; however, localized plastic deformation of the soft base might take place when the load is too large. Therefore, the Zamak5 base, IN625 steel inlay and sheets were all treated as deformable bodies in the analysis.

For the interface between the inlays and zinc base, the joining condition was configured by "Interaction > Create > Contact > Mechanical > Cohesive Behavior > Specify Stiffness Coefficients" in Abaqus [22], where the traction force in unit separation K was set to 1.623 N/mm^3. The quadratic traction damage criterion was chosen. The nominal stress in the pure normal mode σ_n was set to 0.138 N/mm^2, and the nominal stress in the first shear direction σ_s was set to 0.62 N/mm^2.

Table 1
Mechanical parameters of the materials

	Density ρ [kg/m^3]	Young's modulus E [GPa]	Poisson's ratio v	Yield stress σ_s [MPa]
Al6061	2.75×10^{-6}	69.9	0.33	182
SUS304	7.93×10^{-6}	194	0.3	236
IN625	8.40×10^{-6}	205	0.308	682
Zamak5	6.6×10^{-6}	98	0.28	197

4 Fabrication Of The Tool

4.1 Inlay design

Figure 5a) illustrates the von Mises stress distribution in the lower die block with a traditional integral structure during the formation of the W-shaped part under a forming load of 100 kN. The stress is concentrated around the middle ridge, as shown by the fan-shaped outline. The maximum stress value reaches 269 MPa, which is larger than the yield strength of Zamak5 (197 MPa); therefore, plastic deformation will occur in the region and then cause forming defects. To prevent this phenomenon, the ridge needs to be strengthened. It should be noted that the strengthening effect of inlay(s) is most effective when the regions withstand compressive stress – the general stress mode in most conditions of press working; however, the von Mises stress does not distinguish between the tensile and compressive stresses.

The design scheme for a specific inlay is actually arbitrary. As mentioned, the working surfaces, being geometrically consistent with the workpiece, should be smooth and dense, while the areas joining the zinc base should have a rugged pattern to increase the reliability of die blocks. In the current study, bar-shaped steel inlays, according to the stress distributions, are embedded into the ridges (Fig. 3). Three inlay types with representative bottom geometries were designed (Fig. 6) and named “Cross”, “Transverse” and “Longitudinal”. The die block fabricated by Zamak5 without an inlay was named “Pure”.

Figure 5b) shows the stresses within the reinforced die block under the same forming load. The maximum stress is still located in the middle ridge, but the value increases to 473 MPa, which is less than the yield strength of IN625 (682 MPa); thus, there will be no plastic deformation in the die block during forming.

4.2 Fabrication of die blocks

The die blocks were made by a sand-casting process, as shown in Fig. 7. Prototypes of the upper and lower blocks used for casting, which are the exact geometric replicas of the final die blocks, were made of R4600 photosensitive resin by the 3DP process (Fig. 7a)). The draft angle on both sides of the blocks was 5°, and a processing allowance of 1 mm was reserved on the working surfaces. Figure 7b-c) shows the sand tank and the cavity of the transfer mold obtained by burying the resin prototypes into the sand tank.

During casting, the raw materials of Zamak5 were heated to approximately 460 ℃ in a medium-frequency induction heating furnace for melting. For the die blocks with inlays, the cleaned SLM inlays were fixed in the mold cavity by dowel pins before pouring the melted metal to avoid position deviation under the impact of liquid metal. Figure 7d) shows the finished die blocks after removal from the casting mold.

Although the steel inlays can hold their shape and dimension well during casting processes, the casted rough blocks, together with the inlays, should be machined and polished to meet the accuracy and

surface quality requirements, as shown in Fig. 8a-b). Then, the die blocks were assembled to construct the final tool for stamping, as shown in Fig. 8c).

5 Forming Results And Discussion

5.1 Effect of inlays on sheet deformation

Figure 9 shows the W-shaped parts formed with different die blocks. The new tool can stably and reliably form sheet metal parts. Figure 10 shows the load–stroke curves of the experiments and simulations. Apparently, the influence of inlays on the forming load is very small.

To clearly examine the details of the formed parts, macro photography was used to extract the outline information of the round corners in the middle of the W-shaped parts, as shown in Fig. 11.

Figure 12 compares the inner outlines of the corners under the maximum forming loads of 30 kN, 50 kN and 80 kN. Figure 13 presents the bending radii under various forming conditions. The geometric deviations of the parts formed by the reinforced dies are smaller than those formed by the die without inlays, meaning that the inlays can improve the forming accuracy. With increasing maximum load, the bending radii and shape deviations decrease. Moreover, the radii of the parts formed by the die block reinforced by the “Longitudinal" inlay are closer to the expected value of 1 mm.

Figure 14 shows the springback of the middle corners under various conditions, determined by subtracting the desired value of the bending angle (77.32°) from the measurements. With the increase in maximum forming loads, the springback obviously decreases; meanwhile, under the same load, the springback of the parts formed by the reinforced dies is less than that formed by the “Pure” die. With the increase in load, the springback change in the parts formed by the “Pure” die block is the largest, indicating that the reinforced die blocks are more stable.

5.2 Analysis of tool deformation and joining strength

Figure 15 illustrates the vertical deformation of the lower die blocks under a forming load of 100 kN. The displacements of the block without an inlay, as well as the deformation area, are larger than those of the reinforced block.

For the die blocks with inlays, Fig. 13 shows that the bending radii formed with the “Transverse” inlay are the largest, while those formed with the “Longitudinal” inlay are the smallest, indicating that the latter has the best forming accuracy. This is mainly attributed to the difference in the structural stiffness of inlays. Figure 16 shows the simulated deformations of the three inlays under the same loading conditions, where a uniform pressure of 100 MPa is applied on the top surfaces, with the bottom surfaces fixed. The results prove that the “Longitudinal” inlay has the largest deformation resistance, while the “Transverse” inlay is the weakest.

Figure 17 shows the simulated interfacial bonding strengths. When the damage parameter CSQUADSCRT is 1, the maximum strength is reached, and the bonding stiffness degrades to zero. According to the results, the maximum damage to the “Cross”, “Transverse” and “Longitudinal” inlays is very small; thus, the joining condition is reliable.

5.3 Wear of the die blocks

In addition to low strength, low wear resistance is also a typical drawback of soft tools. The Archard wear model gives the main factors impacting wear [22]:

$$w = \int K\frac{Pv}{H}dt$$

1

where w is the wear depth; P is the contacting force; v is the sliding velocity; H is the hardness of the tool; dt is the time increment; and K is the experimental correction coefficient, which was set to 5×10^{-5} in the calculation.

According to the model, the hardness of the die block is the key factor that affects the wear resistance. A digital Vickers hardness tester (Model 200HVS-5) was used to examine the surface hardness of the inlays and zinc alloys. The results are presented in Table 2.

Table 2
Average surface hardness values of the inlays and zinc alloy before and after casting

Materials & Treatment	SLM IN625 inlay		Zamak5	
	Before Casting	After Casting	Before Casting	After Casting
Surface hardness (HV)	237	244	97	140

After casting, the surface hardness of IN625 inlays slightly increases from 237 HV to 244 HV, while that of Zamak5 increases from 97 HV to 140 HV. The reason why the hardness of the zinc alloy increases more after casting is that a fine-grain structure is formed during rapid cooling in casting, leading to an increase in the mechanical properties.

Apparently, steel inlays with higher hardness will improve the wear resistance of die blocks. Figure 18 compares the wear distributions on the middle corner surfaces of the lower die blocks after forming 1000 Al6061 sheets. An Abaqus subroutine was developed to obtain the velocity and pressure of the nodes; the wear values were calculated by the Archard model. The maximum wear value of the Zamak5 block without an inlay is 1.19×10^{-4} mm, while that of the strengthened blocks is reduced to 5.06×10^{-5} mm.

6. Conclusions

This paper examined a new structure of zinc-based soft dies for rapid, economical and precise sheet metal forming, where the weak features on the die blocks are reinforced by hard steel inlays made by SLM additive manufacturing. A complete technical route for developing tools was established, and a W-shaped sheet metal part was employed to verify the concept. The experimental and numerical analysis results proved that smaller radii and clearer localized geometric features can be obtained on the workpiece with the new tool, while the springback is smaller and the wear resistance of the die blocks is higher.

By exploiting the ability of AM technologies, the inlays can adopt a flexible form integrating the “structure” and “function” requirements and then guarantee the forming quality and reliability of the tool system. The new tool possesses the characteristics of both traditional hard and soft dies for sheet metal forming, and the overall cost can be controlled within a reasonable level.

Declarations

Authors’ contributions Tong Wen: Conceptualization, Methodology, Writing - original draft & editing, Resources, Supervision, Project administration, Funding acquisition. Longqin Liu: Methodology, Experiment, Software, Validation, Formal analysis, Investigation, Data processing, Writing - original draft, Visualization. Xu Wang: Software, Visualization, Data processing, Writing & drawing. Yu Zheng: Experiment, Visualization, Data processing. Fan Yang: Experiment, Software. Yin Zhou: Experiment, Software.

Funding This work was supported by the Natural Science Foundation of Chongqing (cstc2020jcyj-msxmX0420), the Fundamental Research Funds for the Central Universities (2020CDJ-LHZZ-062), and the Chongqing Key Laboratory of Metal Additive Manufacturing (3D Printing), Chongqing University.

Data availability The datasets generated and analyzed during the current study are available from the corresponding author on reason-able request.

Compliance with ethical standards

Conflict of interest The authors declare that they have no conflict of interest.

Ethical approval The research does not involve human participants or animals and the authors warrant that the paper fulfills the ethical standards of the journal.

Consent to participate It is confirmed that all the authors are aware and satisfied of the authorship order and correspondence of the paper.

Consent to publish All the authors are satisfied that the last revised version of the paper is published without any change.

Code availability Not applicable.

References

1. He F, Zheng T, Ning W, Hu Z (2000) Explosive forming of thin-wall semi-spherical parts. Materials Letters 45(2):133-137
2. Yarlagadda P, Ilyas IP, Christodoulou P (2001) Development of rapid tooling for sheet metal drawing using nickel electroforming and stereolithography processes. J Mater Process Technol 111(1-3):286-294
3. Yoo S, Walczyk DF (2005) Advanced design and development of profiled edge laminae tools. J Manuf Process 7(2):162-173
4. Zhang H, Wang G, Luo Y, Nakaga T (2001) Rapid hard tooling by plasma spraying for injection molding and sheet metal forming. Thin Solid Films 390(1-2):7-12
5. Male AT, Chen Y, Pan C, Zhang Y (2003) Rapid prototyping of sheet metal components by plasma-jet forming. J Mater Process Technol 135(2-3):340-346
6. Kyrsanidi AK, Kermanidis TB, Pantelakis SG (2000) An analytical model for the prediction of distortions caused by the laser forming process. J Mater Process Technol 104(1-2):94-102
7. Bachmann AL, Dickey MD, Lazarus N (2020) Making light work of metal bending: Laser forming in rapid prototyping. Quantum Beam Sci 4(4)
8. Shulkin LB, Posteraro RA, Ahmetoglu MA, Kinzel GL, Altan T (2000) Blank holder force (BHF) control in viscous pressure forming (VPF) of sheet metal. J Mater Process Technol 98(1):7-16
9. Liu J, Ahmetoglu M, Altan T (2000) Evaluation of sheet metal formability, viscous pressure forming (VPF) dome test. J Mater Process Technol 98(1):1-6
10. Liu Q, Lu C, Fu W, Tieu K, Li M, Gong X (2012) Optimization of cushion conditions in micro multi-point sheet forming. J Mater Process Technol 212(3):672-677
11. Li Y, Shi Z, Yang Y, Lin JG, Said R (2018) Experimental and numerical study of creep age forming of AA2050 plates with sparse multi-point flexible forming tool. 17th International Conference on Metal Forming, Sep 16-19, Toyohashi, Japan
12. Wu S, Ma Y, Gao L, Zhao Y, Rashed S, Ma N (2020) A novel multi-step strategy of single point incremental forming for high wall angle shape. J Manuf Process 56:697-706
13. Milutinovic M, Lendjel R, Balos S, Zlatanovic DL, Sevsek L, Pepelnjak T (2021) Characterisation of geometrical and physical properties of a stainless steel denture framework manufactured by single-point incremental forming. Journal of Materials Research and Technology 10:605-623
14. Wen T, Chen X, Zheng J, Qing J, Tang Z (2017) Multi-directional incremental sheet forming-a novel methodology for flexibly producing thin-walled parts. Int J Adv Manuf Technol 91(5-8):1909-1919
15. Jurisevic B, Sajn V, Kosel F, Junkar M (2008) Introduction of laminated supporting tools in water jet incremental sheet metal forming. Int J Adv Manuf Technol 37(5-6):496-503
16. Cui X, Mo J, Li J, Zhao J, Zhu Y, Huang L, Li Z, Zhong K (2014) Electromagnetic incremental forming (EMIF): A novel aluminum alloy sheet and tube forming technology. J Mater Process Technol 214(2):409-427

17. Wang Z, Cai S, Chen J (2020) Experimental investigations on friction stir assisted single point incremental forming of low-ductility aluminum alloy sheet for higher formability with reasonable surface quality. J Mater Process Technol 277
18. Durgun I, Kus A, Sakin A, Unver E, Jagger B, Doruk E, Findik F (2016) Experimental investigation of sheet metal forming using a recyclable low melting point alloy tool. Materials Testing 58(5):475-480
19. Kuo CC, Li M (2017) Development of sheet metal forming dies with excellent mechanical properties using additive manufacturing and rapid tooling technologies. Int J Adv Manuf Technol 90(1-4):21-25
20. Kleiner M, Curbach M, Tekkaya EA, Ritter R, Speck K, Trompeter M (2008) Development of ultra high performance concrete dies for sheet metal hydroforming. Production Engineering 2(2):201-208
21. Schuh G, Bergweiler G, Bickendorf P, Fiedler F, Colag C (2020) Sheet metal forming using additively manufactured polymer tools. Procedia CIRP 93:20-25
22. Hibbitt R., Karlsson D., Sorensen C (2006) ABAQUS User's Manual (version 6.3). Pawtucket, RI.

Figures

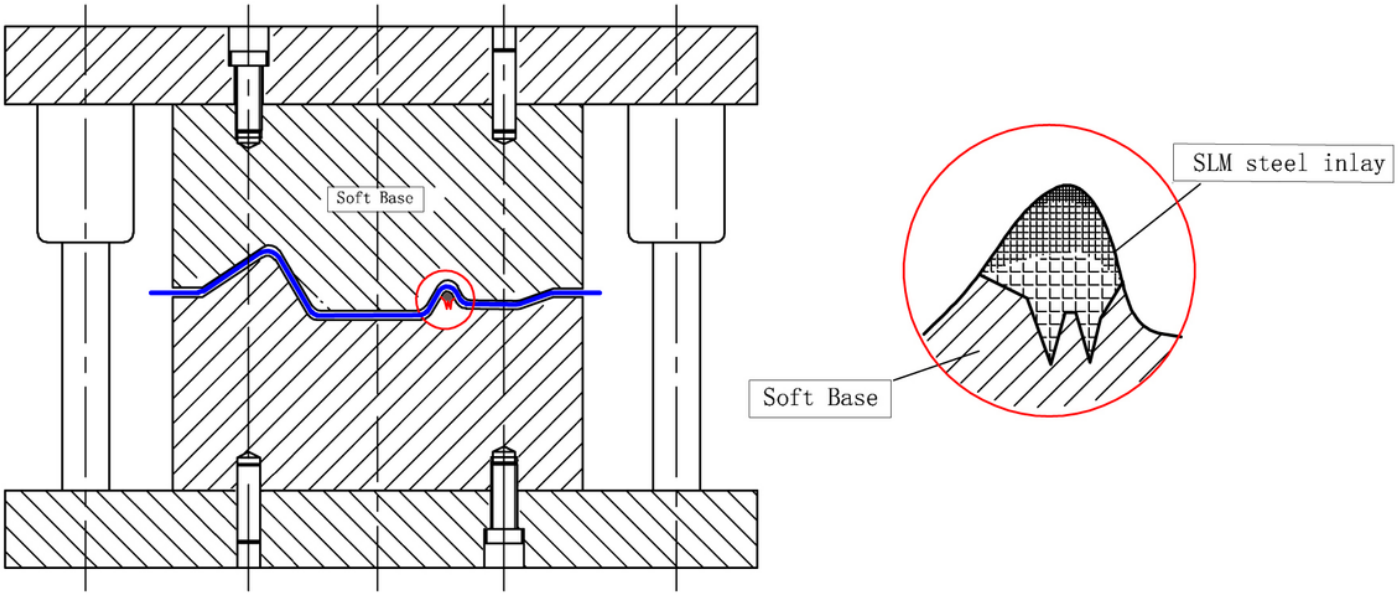

Figure 1

Schematic diagram of a zinc-based rapid die for sheet metal-forming reinforced by steel inlays

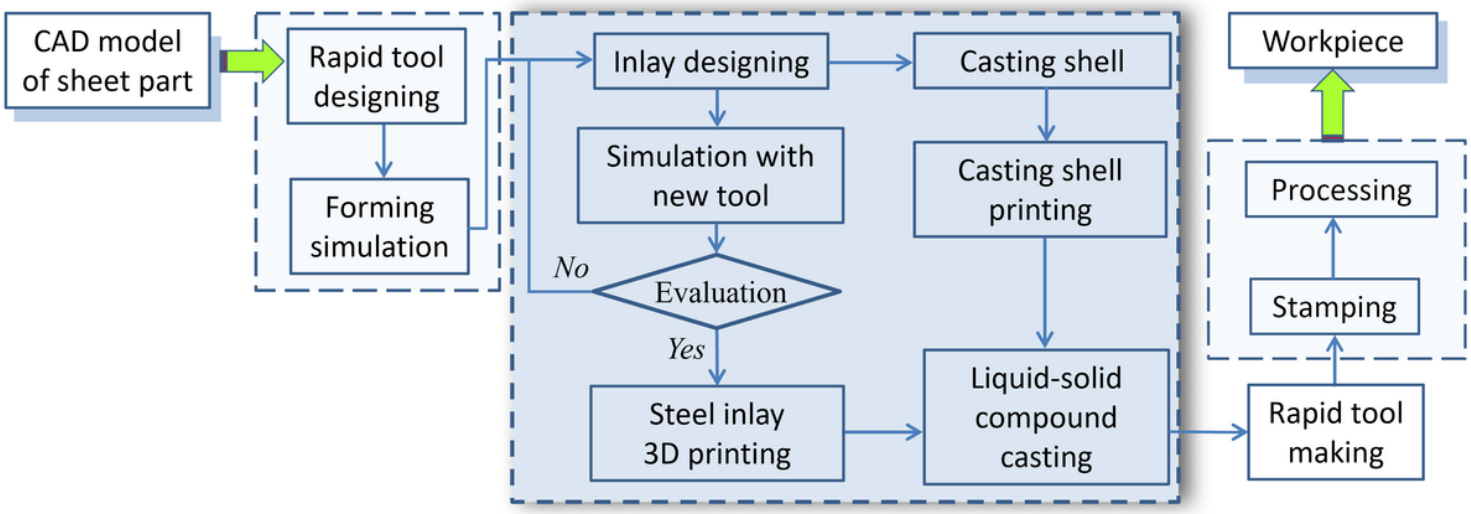

Figure 2

Technical route for fabricating rapid tools for forming sheet metal reinforced by SLM steel inlays

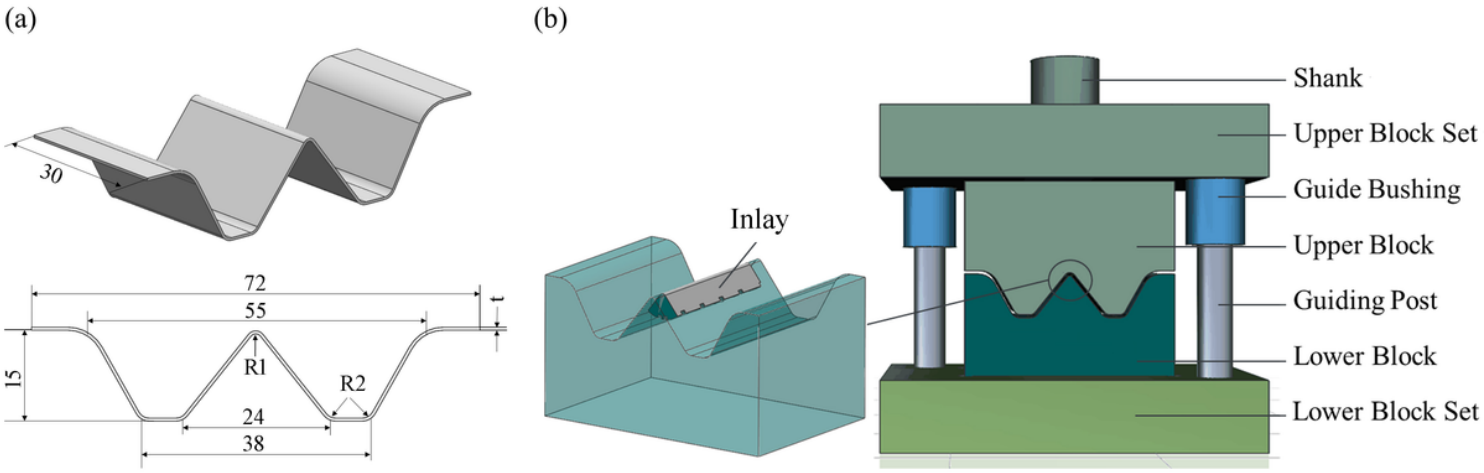

Figure 3

(a) Target part and (b) stamping die design

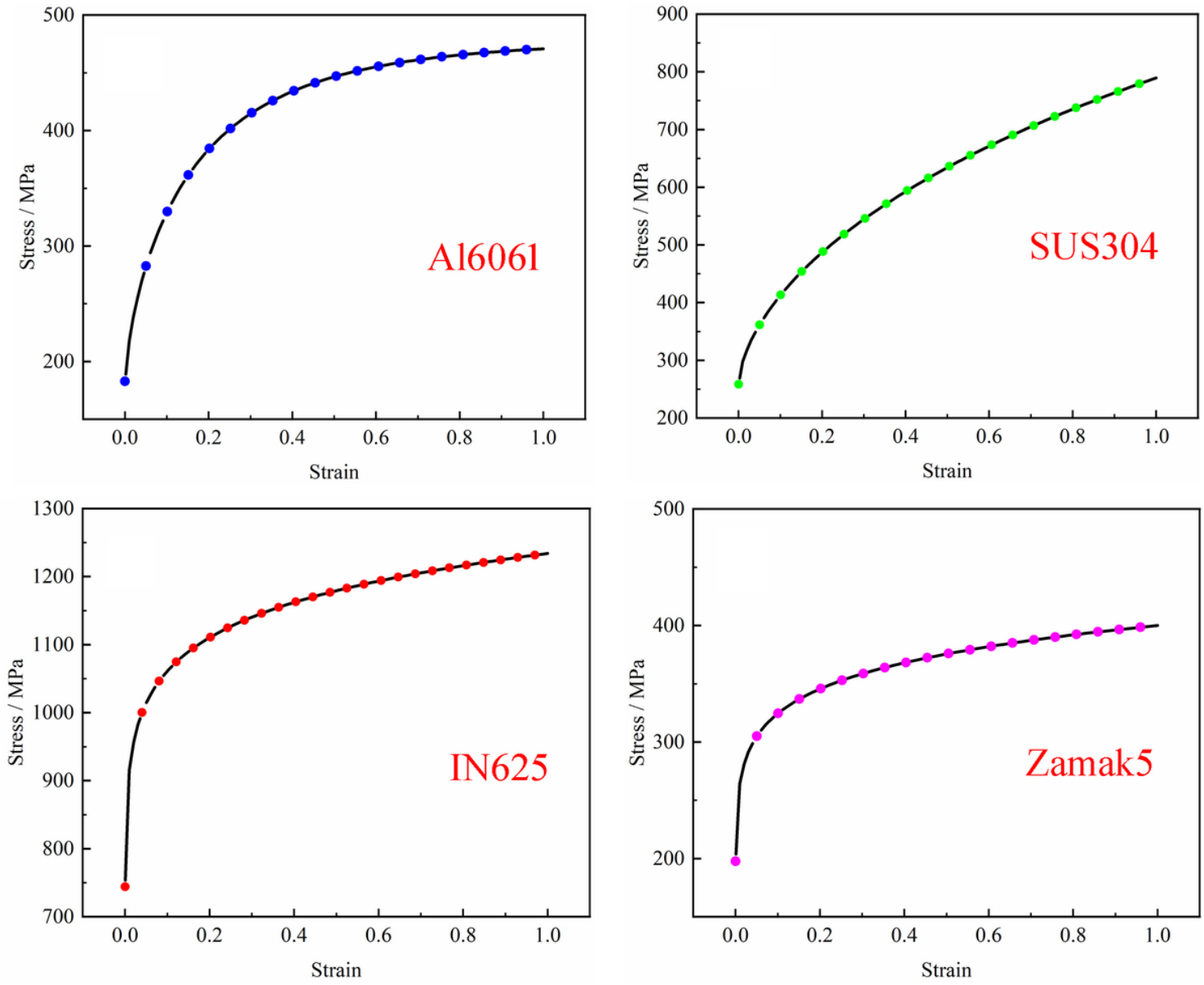

Figure 4

Stress–strain curves of the materials in the experiment

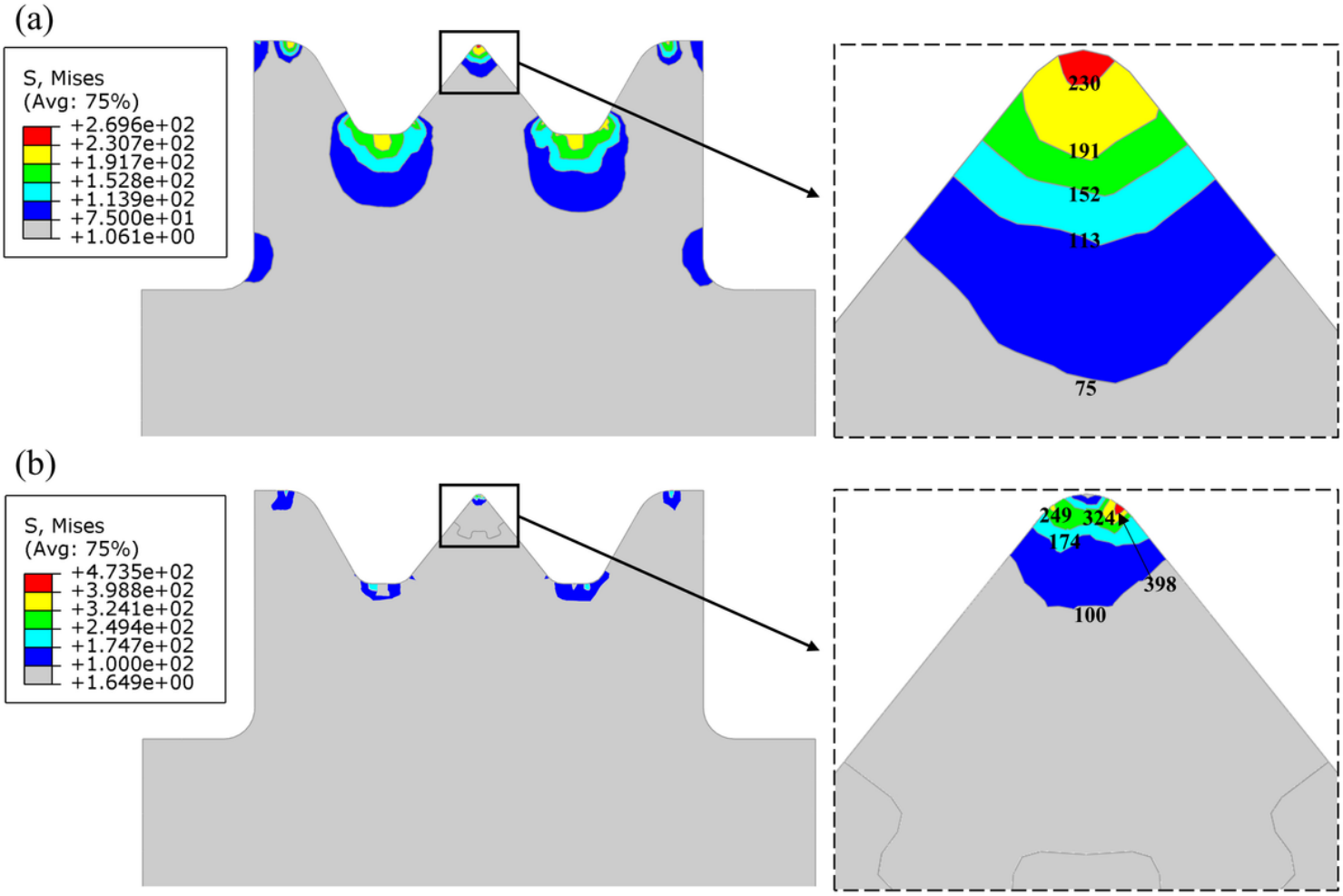

Figure 5

Stress distributions within the die blocks under the maximum load of 100 kN: (a) without an inlay and (b) with an inlay

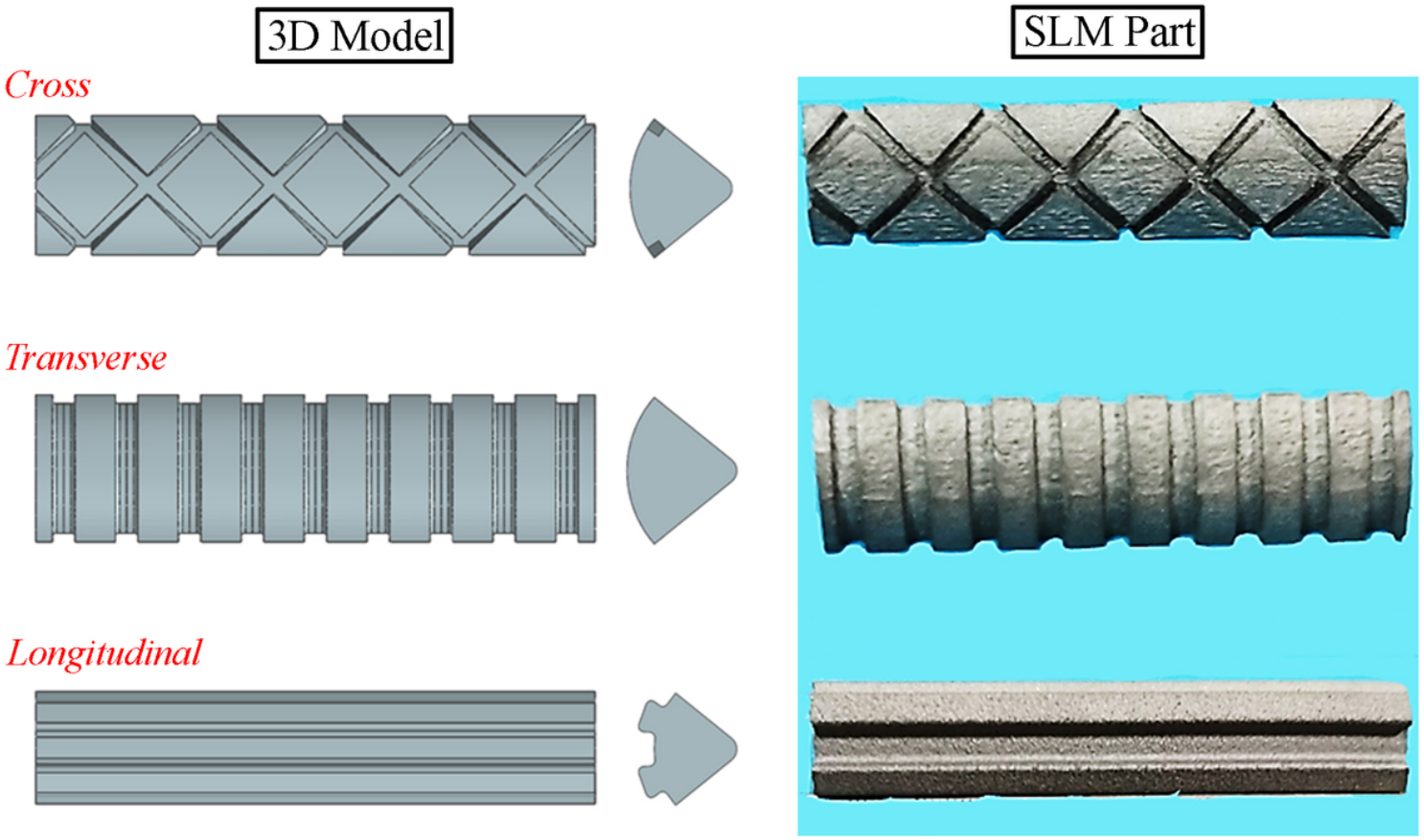

Figure 6

Three types of joining patterns of the inlays

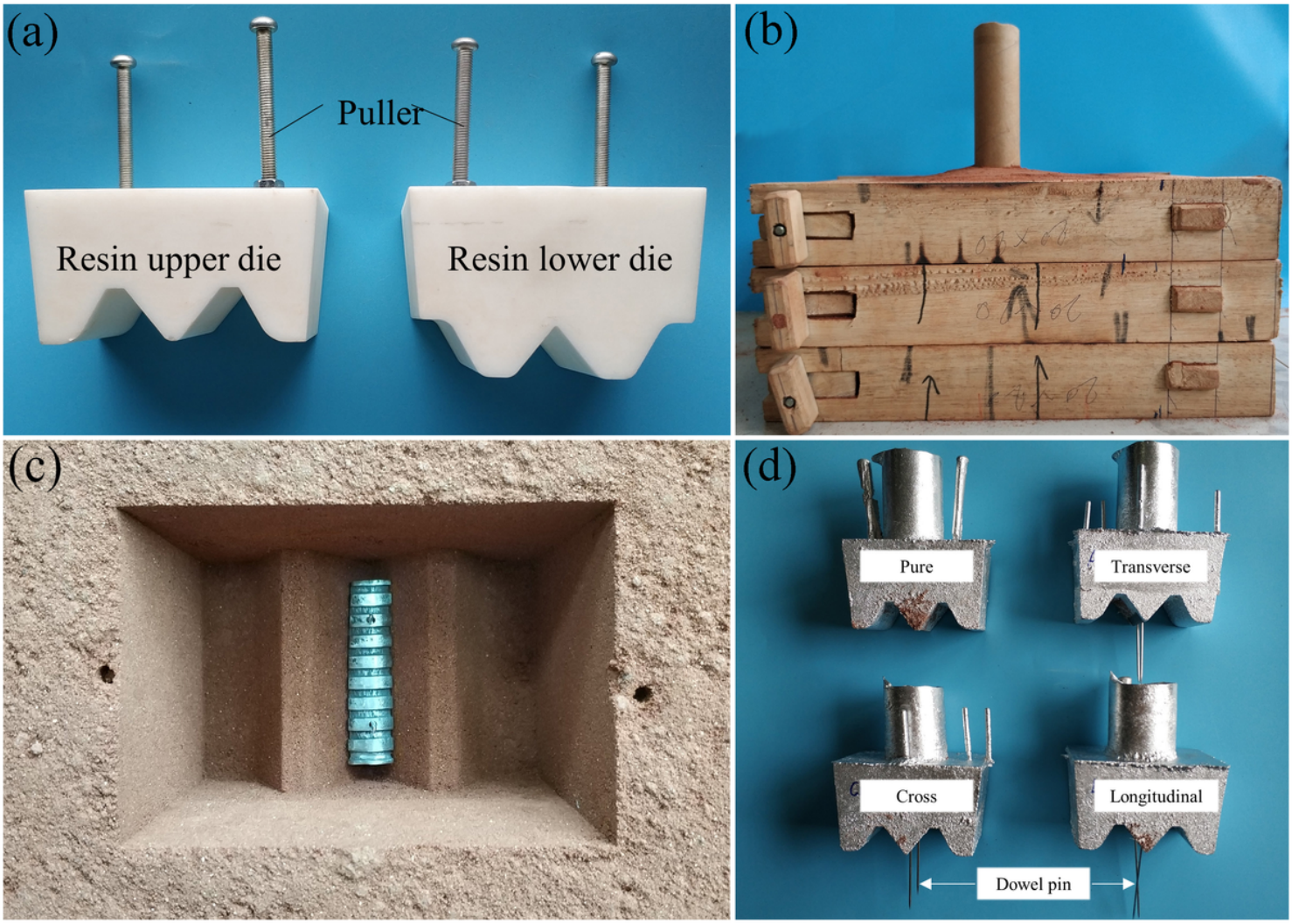

Figure 7

Casting procedure of the die blocks: (a) resin prototypes; (b-c) sand box and mold for casting; and (d) finished blocks

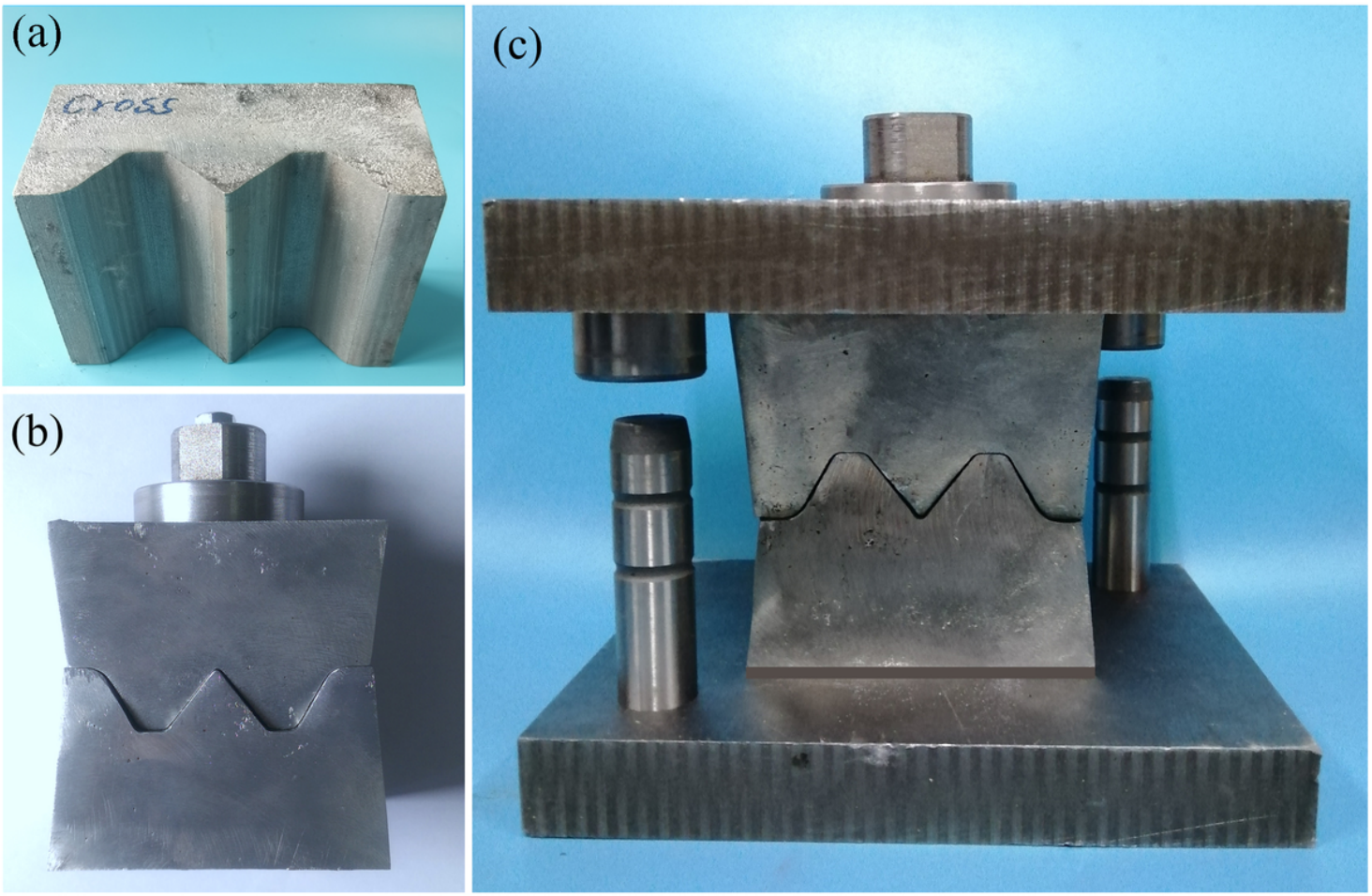

Figure 8

Preparation process after casting: (a) original block; (b) machining and polishing; and (c) tool assembly

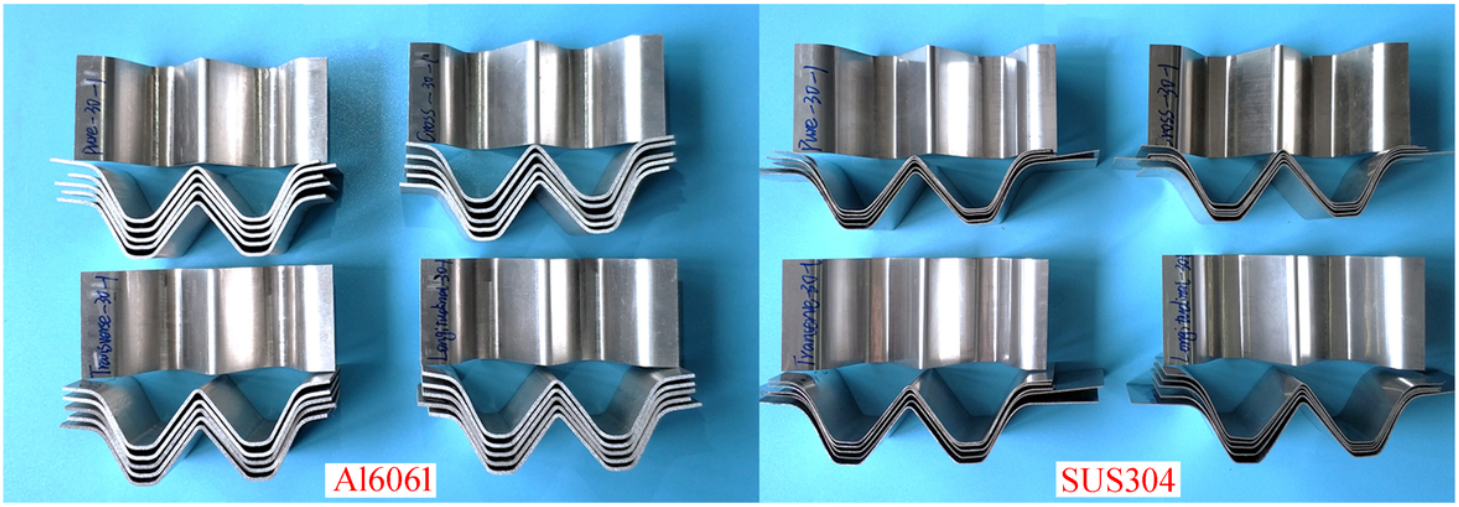

Figure 9

Formed parts of Al6061 and SUS304 sheets using die blocks with/without inlays

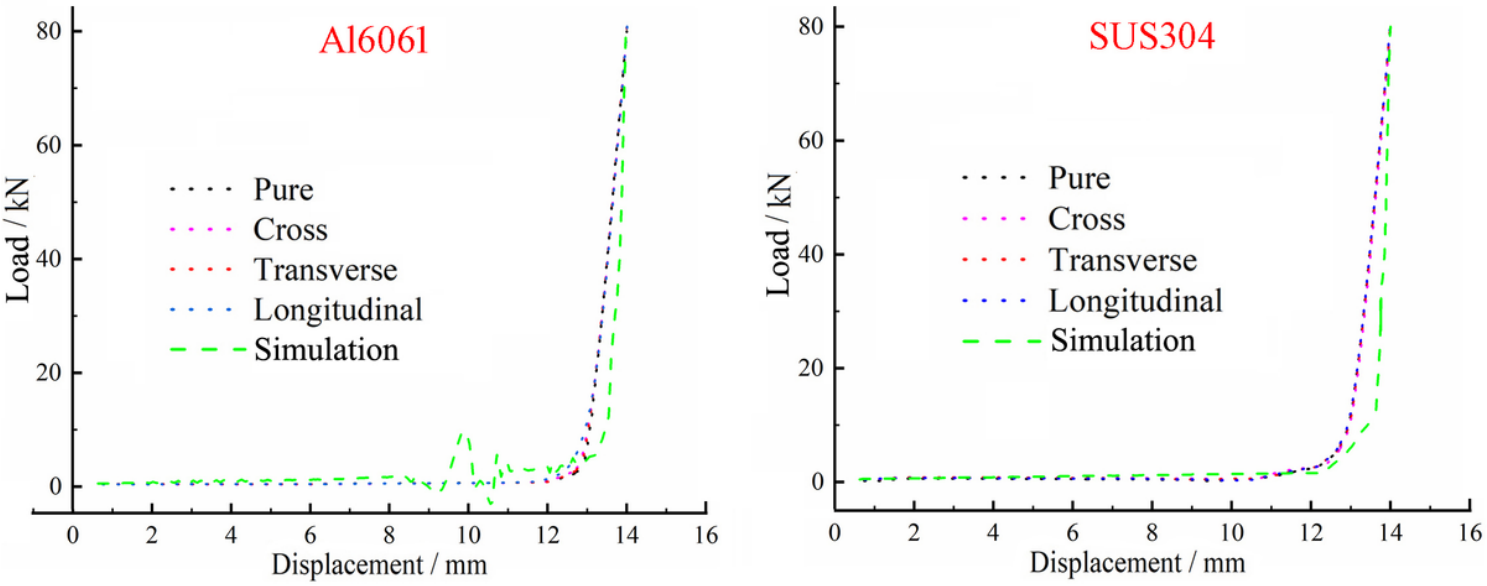

Figure 10

Load–stroke curves with a maximum load of 80 kN

Figure 11

Outlines of the formed corners extracted by macro photography

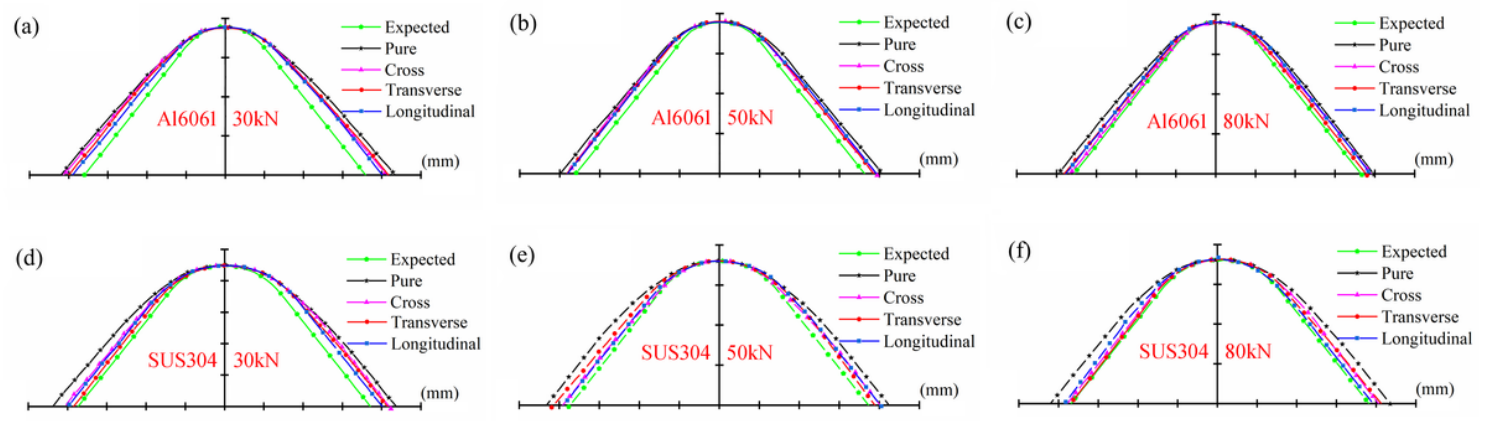

Figure 12

Comparison of the inner outlines of the middle corners formed under various conditions

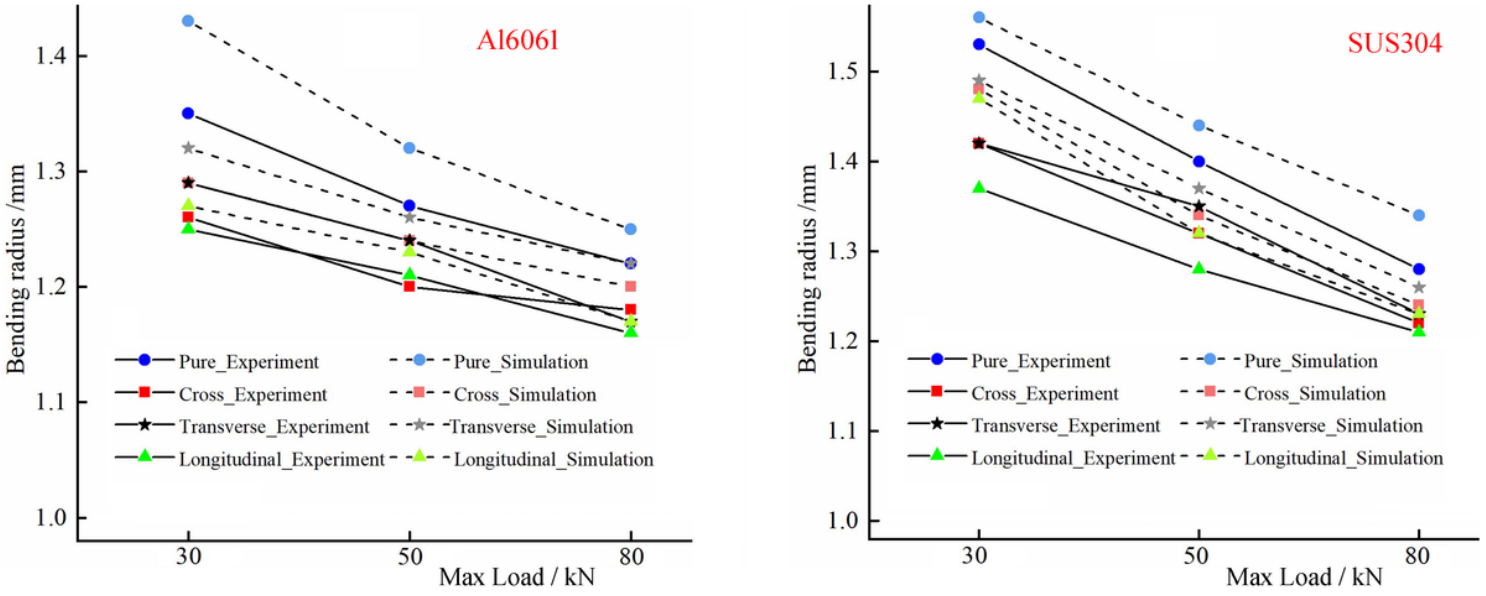

Figure 13

Inner bending radii of the middle corners formed under various conditions

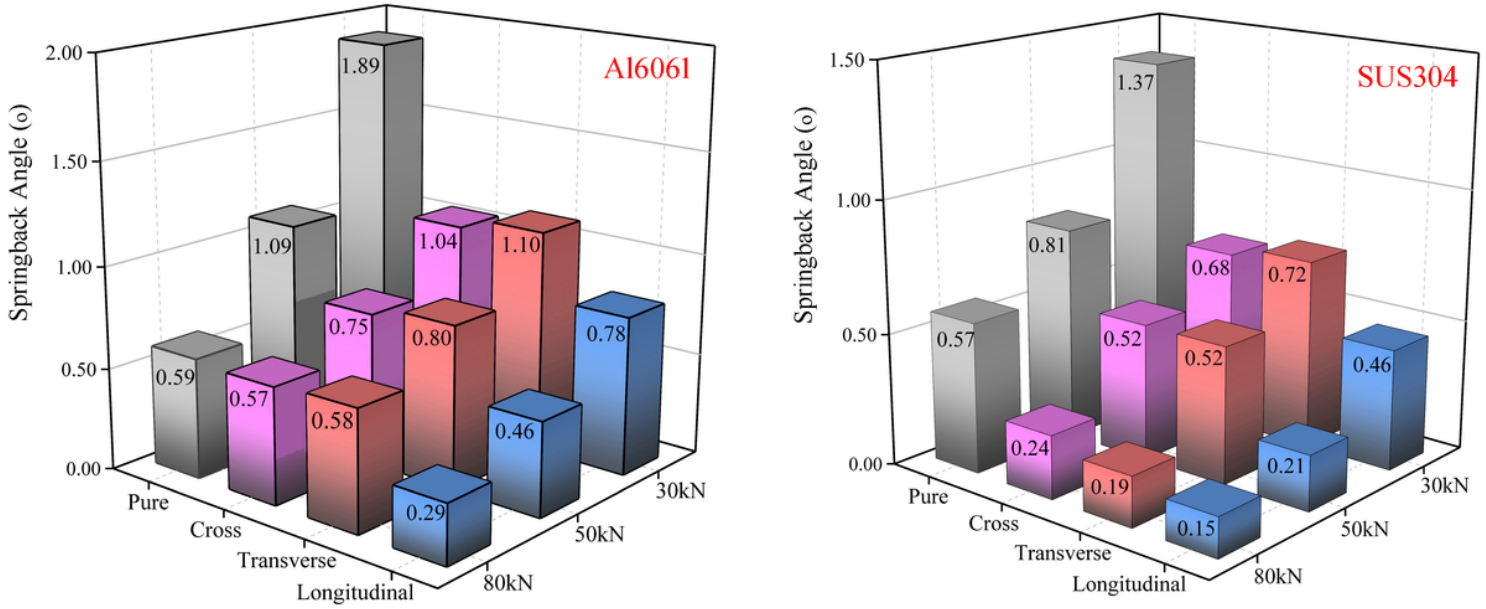

Figure 14

Experimental springback values of the middle corners under different maximum forming loads

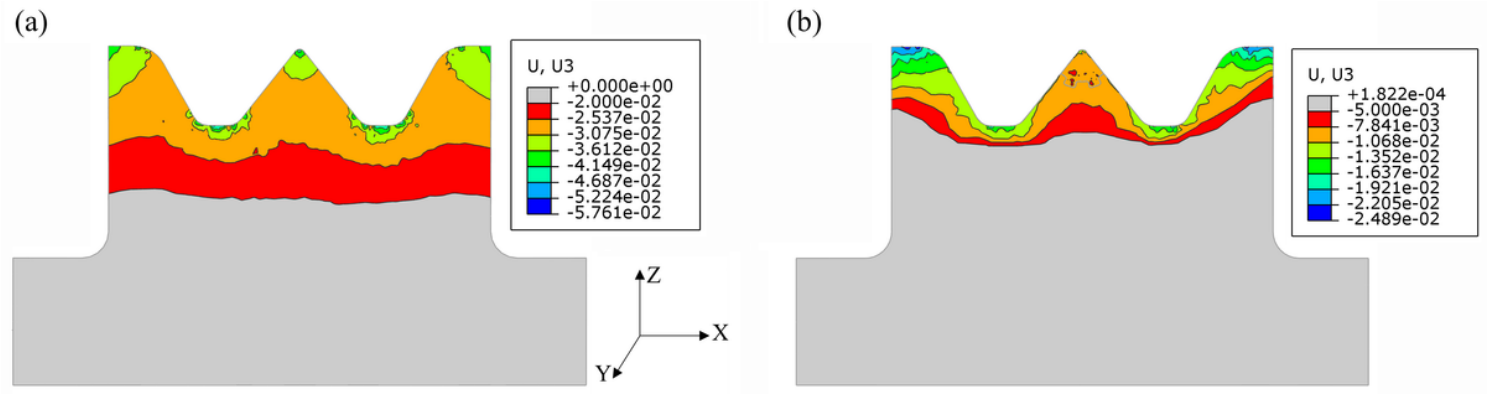

Figure 15

Vertical displacement distributions under a load of 100 kN: (a) without inlays and (b) with longitudinal inlays

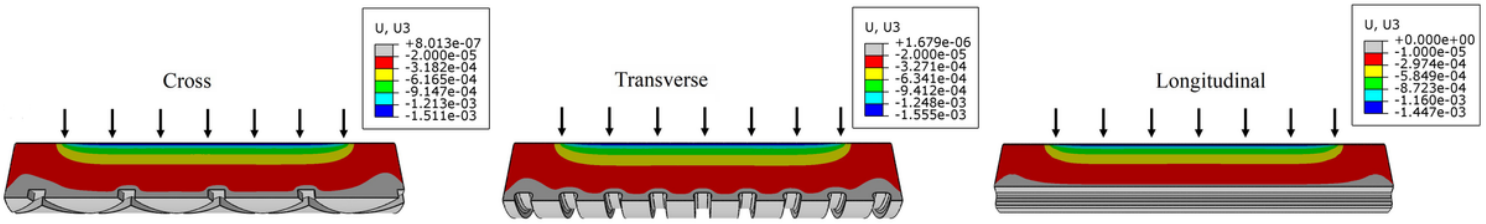

Figure 16

Analysis of the deformation resistance of inlays

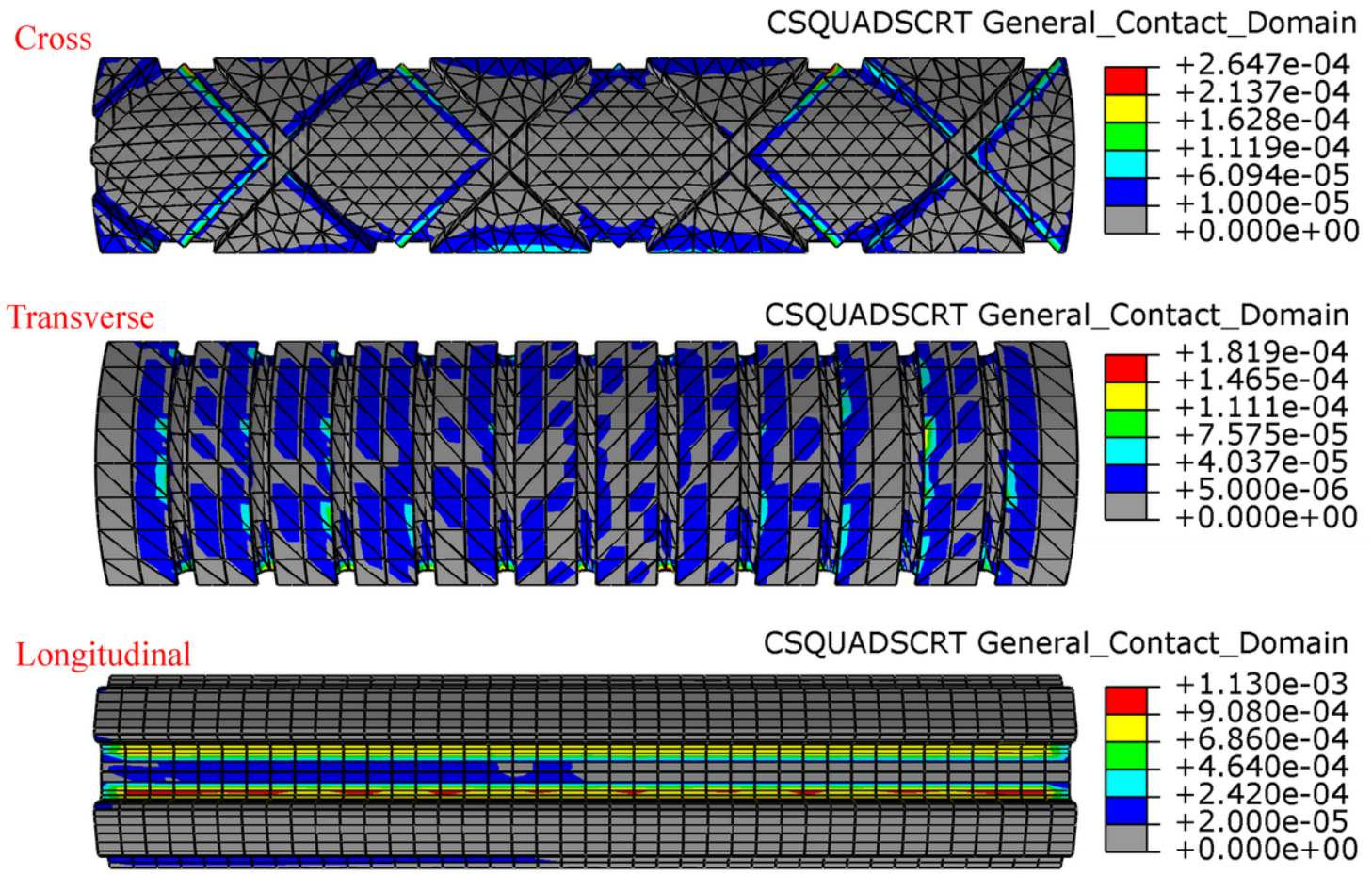

Figure 17

Comparison of the interfacial bonding strengths under a load of 100 kN

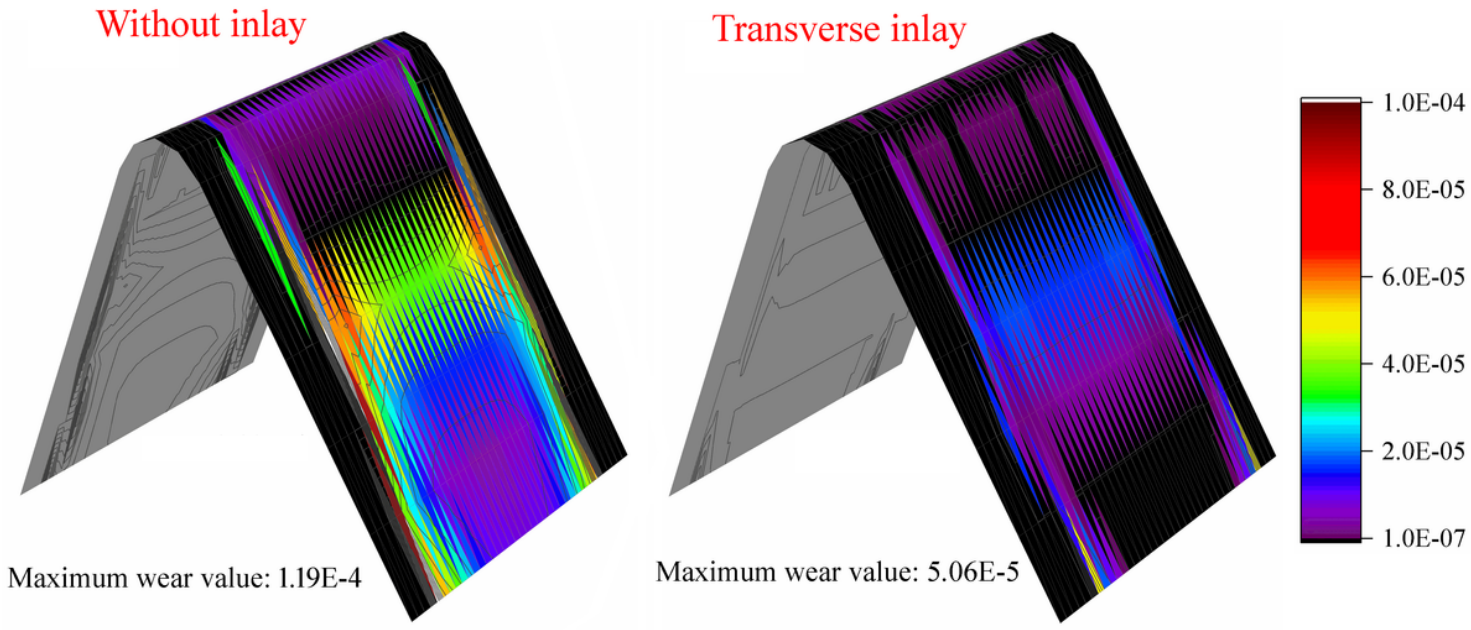

Figure 18

Surface wear on the middle corners of the lower die blocks after forming 1000 Al6061 sheets under a maximum load of 50 kN